Structures Linking Microfilament Bundles to the Membrane at Focal Contacts

Steven J. Samuelsson,* Paul W. Luther,* David W. Pumplin,‡ and Robert J. Bloch*

*Departments of Physiology and ‡Anatomy, University of Maryland School of Medicine, Baltimore, Maryland 21201

Abstract. We used quick-freeze, deep-etch, rotary replication and immunogold cytochemistry to identify a new structure at focal contacts. In *Xenopus* fibroblasts, elongated aggregates of particles project from the membrane to contact bundles of actin microfilaments. Before terminating, a single bundle of microfilaments interacts with several aggregates that appear intermittently over a distance of several microns. Aggregates are enriched in proteins believed to mediate actin-membrane interactions at focal contacts, including β_1-integrin, vinculin, and talin, but they appear to contain less α-actinin and filamin. We also identified a second, smaller class of aggregates of membrane particles that contained β_1-integrin but not vinculin or talin and that were not associated with actin microfilaments. Our results indicate that vinculin, talin, and β_1-integrin are assembled into distinctive structures that mediate multiple lateral interactions between microfilaments and the membrane at focal contacts.

FOCAL contacts are specialized structures where actin filaments converge and terminate at the plasma membrane (16, 32, 44, 63, 65). Interactions between the membrane and microfilaments involve several proteins that are concentrated at focal contacts, including integrin (e.g., references 17, 21, 22; reviewed in 1, 61) and cytoskeletal proteins such as vinculin (26), talin (13), fimbrin (9), tensin (71), paxillin (68), zyxin (5), and α-actinin (40). Biochemical studies have suggested several ways in which these proteins could anchor microfilaments to the cytoplasmic surface of the plasma membrane at focal contacts. Early studies suggested that particular isoforms of integrin ("CSAT"; 47) bound talin, and that this complex then bound vinculin (35; reviewed in 15). Later studies showed that integrins could also bind α-actinin (53). Thus, integrin could anchor actin filaments indirectly through the actin-binding protein, α-actinin, as well as through talin and vinculin. If both of these mechanisms are important for actin-membrane interactions, one would expect all these proteins to be concentrated at focal contacts.

Structural studies also suggest two models for microfilament-membrane interactions at focal contacts. Focal contacts are several microns long, and individual actin filaments course over this entire distance before terminating (8). These filaments could bind to the membrane laterally as they approach their termini. In this case, vinculin, talin, integrin, and other proteins of focal contacts would be expected to concentrate at many points along the filament length. Alternatively, filaments could attach only at their termini. In this case, the proteins of focal contacts would be expected to occur only at the ends of microfilaments.

Predictions of the relationship between actin microfilaments and the membrane, and of the distribution of proteins at focal contacts, can be tested by ultrastructural methods coupled with immunocytochemistry. We exposed the cytoplasmic surfaces of ventral membrane by mechanical shearing, then used quick-freeze, deep-etch, rotary replication (QFDERR; 33) to study the organization of focal contacts. This method gives en face views of large areas of the plasma membrane, enabling us to characterize the organization of focal contacts in three dimensions. We show (*a*) that actin microfilaments at focal contacts make many lateral connections to the membrane; and (*b*) that these connections occur at distinctive aggregates of particles that contain vinculin, talin and β_1-integrin. Portions of this work have been presented in abstract form (Samuelsson, S. J., P. W. Luther, D. W. Pumplin, J. B. Wade, and R. J. Bloch. 1990. *J. Cell Biol.* 111:300*a*).

Materials and Methods

Cultures

Procedures for culturing myotomal tissue from stage 21-23 *Xenopus laevis* embryos (51) have been described (3, 41). These cultures contain a nonmuscle cell type (37) previously called a fibroblast (10). For simplicity, we also refer to this cell as a fibroblast. At the stage at which we studied fibroblasts, they were nonmotile.

Immunoblots

Xenopus tadpoles were anesthetized in 0.2% Tricaine (Sigma Chemical Co., St. Louis, MO). Their tails were removed, frozen in liquid nitrogen, lyophi-

Dr. Samuelsson's present address is Department of Biophysics, The Johns Hopkins University, Baltimore, MD 21218.

Address correspondence to Dr. Bloch at University of Maryland, School of Medicine, 660 W. Redwood Street, Baltimore, MD 21201.

lized and stored desiccated at −70°C. Lyophilized tails were solubilized by boiling in sample buffer (39) for 5 min, followed by centrifugation. Proteins in the supernate were separated by SDS-PAGE on gels containing either 10% or a 5–15% gradient of acrylamide and transferred electrophoretically to nitrocellulose paper (12). Standard proteins were from Bethesda Research Laboratories (Bethesda, MD). These methods have been described in detail elsewhere (7).

Shearing

Solutions used for shearing and labeling were isotonic for *Xenopus* cells. Cultures on glass coverslips were incubated in 3 mM $ZnCl_2$, 60 mM NaCl, 0.67 mM KCl, 10 mM Pipes, pH 6.0, for 4–5 min (modified from reference 4) to increase the amount of ventral membrane left after shearing. To shear cells open, ice-cold buffer (50 mM Pipes, 10 mM $MgCl_2$, pH 6.0) was sprayed onto the coverslips through an 18 gauge needle. Samples for immunocytochemistry were fixed in 0.5% paraformaldehyde, 75 mM cyclohexylamine, 10 mM $MgCl_2$, 10 mM Pipes, pH 6.5 (41) at 0°C. The fixative was allowed to come to room temperature over 30 min, and was then replaced with 75 mM Tris buffer, 10 mM $MgCl_2$, 10 mM NaN_3, pH 7.2. Nonspecific binding was reduced by incubation in 0.1% BSA in Tris buffer (BSA/Tris: 20 mM Tris, 0.5 M NaCl, 10 mM $MgCl_2$, 10 mM NaN_3, pH 7.4) for 1 h before incubation with antibodies. For experiments that did not involve immunogold labeling, the sheared samples were fixed for 1 h in ice-cold 1.0% glutaraldehyde, 0.25% acrolein in 50 mM Pipes, 10 mM $MgCl_2$, pH 6.5, and then subjected to QFDERR (see below). Samples fixed with this solution and samples fixed with cyclohexylamine plus paraformaldehyde had similar morphology.

Although proteins that were not firmly associated with the membrane at focal contacts were probably removed during shearing, this presents certain advantages. Nearly all of the cytoplasm was removed by shearing, leaving an unobstructed view of the membrane and associated structures. The proteins that remained after shearing were likely to be firmly attached to the focal contact and therefore play an important role in its organization.

Antibodies

Monoclonal anti-vinculin antibody (3–24; mouse ascites fluid from the Developmental Studies Hybridoma Bank, Department of Biology, University of Iowa, Iowa City, IA) was used in immunocytochemistry and immunoblot studies at 3–4 μg/ml. All rabbit antibodies were affinity purified. A rabbit antibody against chicken gizzard vinculin (6) was used at 1–2 μg/ml. Rabbit anti-talin antibody, a gift of Dr. K. Burridge (University of North Carolina, Chapel Hill, NC), was diluted 1,500–2,000× for immunocytochemistry and immunoblot studies. A rabbit antibody against a synthetic, 39-amino acid peptide corresponding to the COOH-terminal cytoplasmic sequence of β_1-integrin (43) was provided by Dr. R. O. Hynes (Massachusetts Institute of Technology, Cambridge, MA). Before use, it was centrifuged briefly and then diluted 1:1,000–1:6,000× for immunocytochemistry and 1:500 for immunoblots. Rabbit antibodies to α-actinin and filamin (69) from chicken gizzard (6) were used at 3.9 μg/ml and 1:500, respectively, for immunocytochemistry and at 2 μg/ml and 1:600 for immunoblots. MOPC 21 (Sigma Chemical Co.) and nonimmune rabbit serum were used at 1.8 and 10–20 μg/ml, respectively.

Immunolabeling

Samples were labeled with primary antibodies (see above), followed by a secondary antibody conjugated to either fluorescein or rhodamine, and then a tertiary antibody adsorbed to colloidal gold (Janssen Life Sciences Products, Olen, Belgium). The final antibody solution was applied at a dilution of 1:6 to 1:9 in 0.1% BSA/Tris, pH 8.3. For double-label experiments, cultures were incubated with both a biotinylated anti-rabbit antibody and a fluoresceinated sheep antibody against mouse immunoglobulins. The final incubation consisted of streptavidin adsorbed to 15-nm gold particles combined with donkey anti-sheep immunoglobulin adsorbed to 5 nm colloidal gold. Appropriate controls showed complete species specificity of these secondary and tertiary reagents. Areas of the samples that showed clear labeling in immunofluorescence were selected for examination at the ultrastructural level.

Electron Microscopy

Samples were subjected to QFDERR in a modified Balzer's apparatus, as described (57). Samples were washed in 5% methanol in D_2O and frozen against a copper mirror at −196°C (55). Most D_2O was removed when the samples passed through a jet of dry N_2 gas as it descended to the freezing surface. Etching (sublimation) occurred over 2–4 h at a stage temperature of −95°C. The evolution of D_2O during etching was monitored with a mass spectrometer (70). After freeze-etching, the stage was cooled to −135°C in a vacuum of $\sim 2 \times 10^{-8}$ Torr, and ~1.2 nm of Pt was applied to the rotating sample from an angle of 20°C. Carbon was then applied at an angle of 90° to the rotating stage.

Replicas were examined with a Zeiss 10CA electron microscope equipped with a goniometer stage. Stereo images were recorded at ±6° of tilt. The micrographs were photographically reversed and printed so that the gold particles appeared white and shadows appeared dark. Some images were printed without photographic reversal, to make it easier to see the 5-nm gold particles. These photographs were digitized using a CCD camera (Photometrics, Tucson, AZ) and traced with a graphics program. The identification of gold particles and actin filaments was confirmed by comparison to the original stereo micrographs.

For quantitative measurements, structures of interest were outlined on electron micrographs (80,000 magnification). Areas were measured with a digitizing tablet and Bioquant software (R & M Biometrics, Nashville, TN).

Results

The major objective of our studies was to characterize the cytoplasmic surface of the membrane at focal contacts of fibroblasts. We exposed this surface by shearing cultured cells with a stream of buffer and used Nomarski optics to select isolated cell membranes that were free of overlying cytoplasm. Subsequent processing for QFDERR (see Materials and Methods; 57) produced stereoscopic images of focal contacts, revealing structures that have not been visualized by more conventional ultrastructural methods. In particular, we observed aggregates of particles that appeared to connect microfilaments to the membrane. Immunocytochemical studies demonstrated that vinculin, talin, and β_1-integrin were concentrated in these aggregates.

Ultrastructure of the Microfilament-Membrane Interface

Focal contacts appeared as areas of ventral membrane where linear bundles of filaments terminate (Fig. 1; see references 2, 4, 16, 25, 32, 44, 49, 50, 64). Filaments were 10.3 ± 0.5 nm in diameter (mean ± SD; not corrected for ~1.2 nm of applied platinum) and showed cross striations with a repeat of 5.7 nm (e.g., Fig. 2–4, 7). Both values identify these structures unambiguously as actin (33).

Although a few actin microfilaments appeared to end directly on the membrane (Fig. 4, *white arrows*), most terminated at elongated aggregates of membrane-associated particles. These structures, which we refer to as "type I aggregates," occurred intermittently along the most distal portions (1–3 μm) of microfilament bundles, where filaments came closest to the membrane (e.g., Fig. 1, *curved arrows*). The aggregates of particles appeared to fill the space between the microfilaments and the membrane and were usually somewhat wider than the bundle itself. This interaction was most clearly seen where small bundles of actin filaments were attached to a series of type I aggregates (Fig. 3). These microfilaments made multiple lateral contacts, instead of single, end-on contacts, with the membrane.

Occasional aggregates of particles appeared in areas of the membrane that lacked microfilaments (e.g., Fig. 1, *open arrows*; Fig. 2, *arrowheads*). We identified most of these structures as type I aggregates because they were of approximately the same size and shape, and were arranged linearly in the membrane. (They also contained proteins typical of

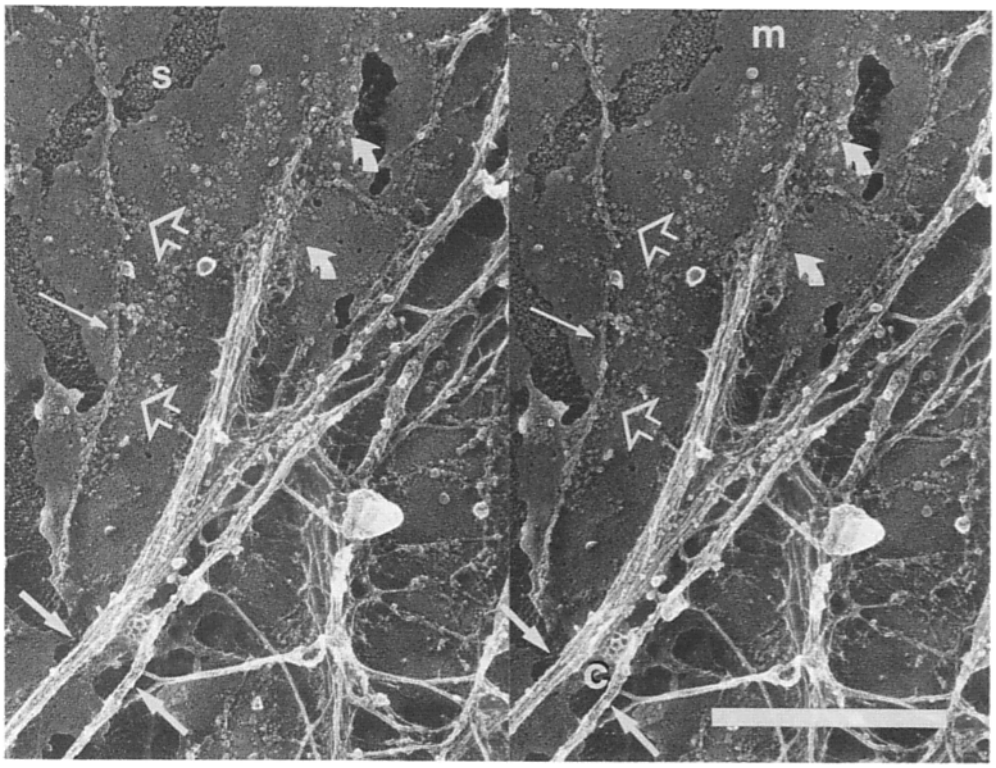

Figure 1. Cytoplasmic membrane surface of focal contacts. Focal contacts in cultured *Xenopus* cells were exposed by shearing with a stream of buffer. After fixation with a mixture of glutaraldehyde and acrolein (see Methods), samples were processed for ultrastructural studies by quick-freeze, deep-etch, rotary-replication. This stereopair shows two bundles of microfilaments (*arrows*), one of which approaches and associates with the membrane. Below and beyond this filament bundle are aggregates of particles that project from the membrane (type I aggregates; *curved arrows*). Parallel to the filament bundle is an area with a linear array of similar particle aggregates (*open arrows*) but with only a single associated microfilament (*thin arrow*), presumably the vestige of a bundle of filaments largely removed by shearing. *M*, membrane; *S*, substrate; *C*, coated vesicle. Bar, 0.5 μm.

focal contacts: see below.) These structures were often in strips of membrane that were raised slightly from the substrate (Fig. 2, *arrowheads*), and occasionally aligned with fibers of extracellular matrix that extended beyond the cell border (Fig. 8 *b*). We believe that these aggregates represent structures that remain at focal contacts when actin microfilaments are removed by shearing.

Because they were more easily studied, type I aggregates that lacked overlying microfilaments were used for morphometric analysis. Particles within the aggregates were heterogeneous in appearance and often occurred in groups of two or three. Clearly defined particles were 11.5 $\pm$ 3.1 nm (range 8.7–15.4; 23 particles from two experiments) in diameter. The average area of type I aggregates was 18.1 $\pm$ 17.5 $\times$ 10^{-3} μm^2 (range 2.8–145 $\times$ 10^{-3} μm^2; 247 aggregates from six experiments). Rather than being normally distributed, aggregates of larger sizes (>5 $\times$ 10^{-3} μm^2) were less common, and a histogram of aggregate size vs number of ag-

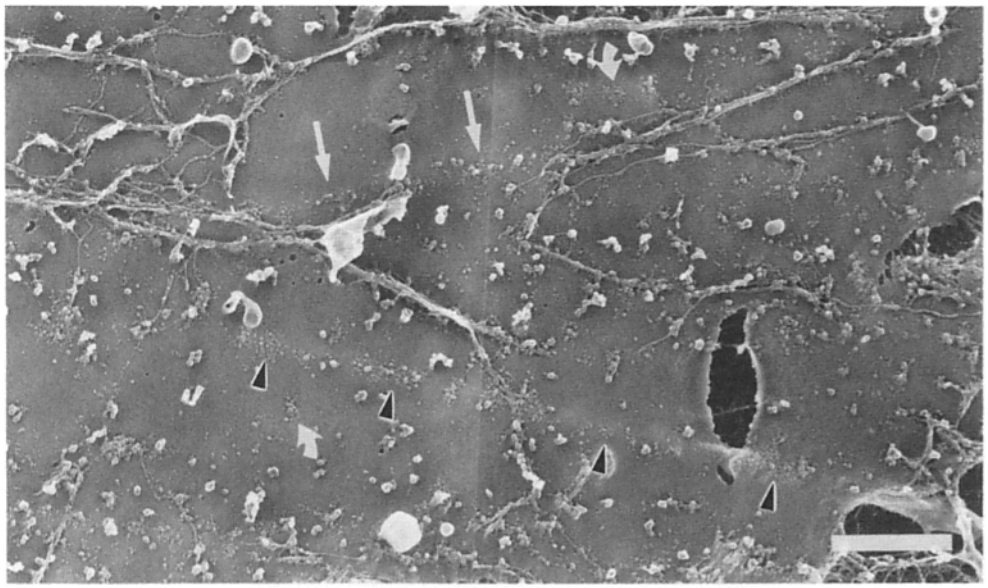

Figure 2. Focal contacts at membrane ridges. This sample, processed as in Fig. 1, shows a linear array of particles (*arrows*) that extends beyond the ends of remaining microfilaments. This array runs along a slight ridge in the membrane, as viewed from the cytoplasm. A similar ridge, also containing aggregates of particles, has no associated microfilaments (*arrowheads*). Type II particle aggregates are also evident between the focal contact regions (e.g., *curved arrows*). Bar, 0.5 μm.

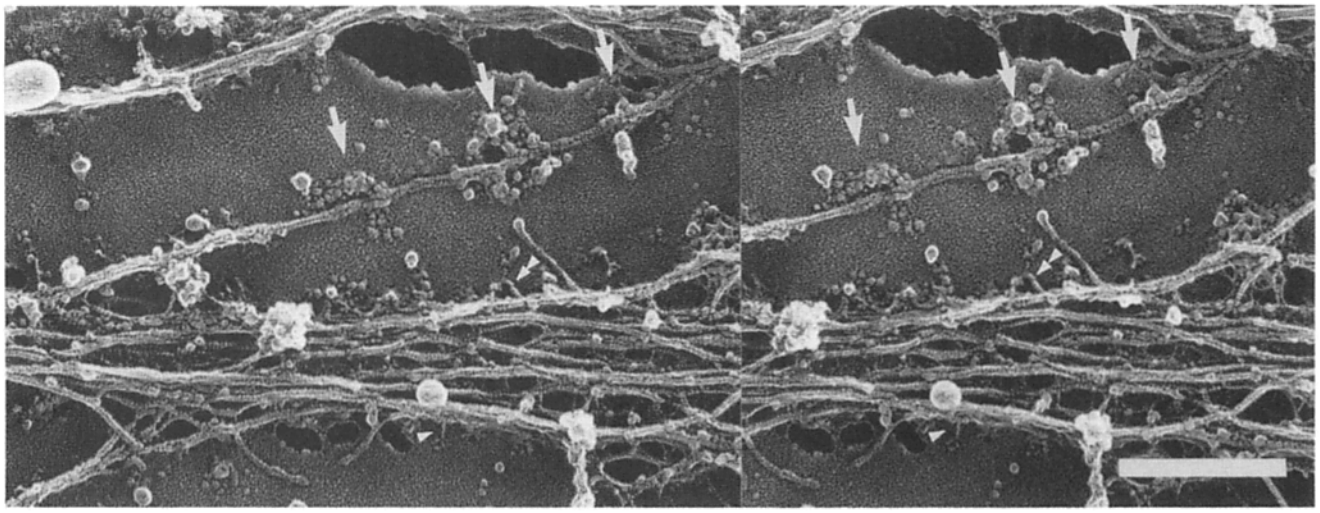

Figure 3. Microfilaments make multiple, lateral attachments to membrane-associated particle aggregates. This stereo pair shows three type I aggregates (*arrows*) associated with a bundle containing at least two actin filaments. Because this association survived the shearing process, it is likely that the actin filaments and aggregates are bound to each other. The lower, larger bundle of actin filaments has examples of both the large filaments (*dual arrowheads*) and small filaments (*arrowheads*) that also link microfilaments and plasmalemma (see Fig. 4). Bar, 0.25 μm.

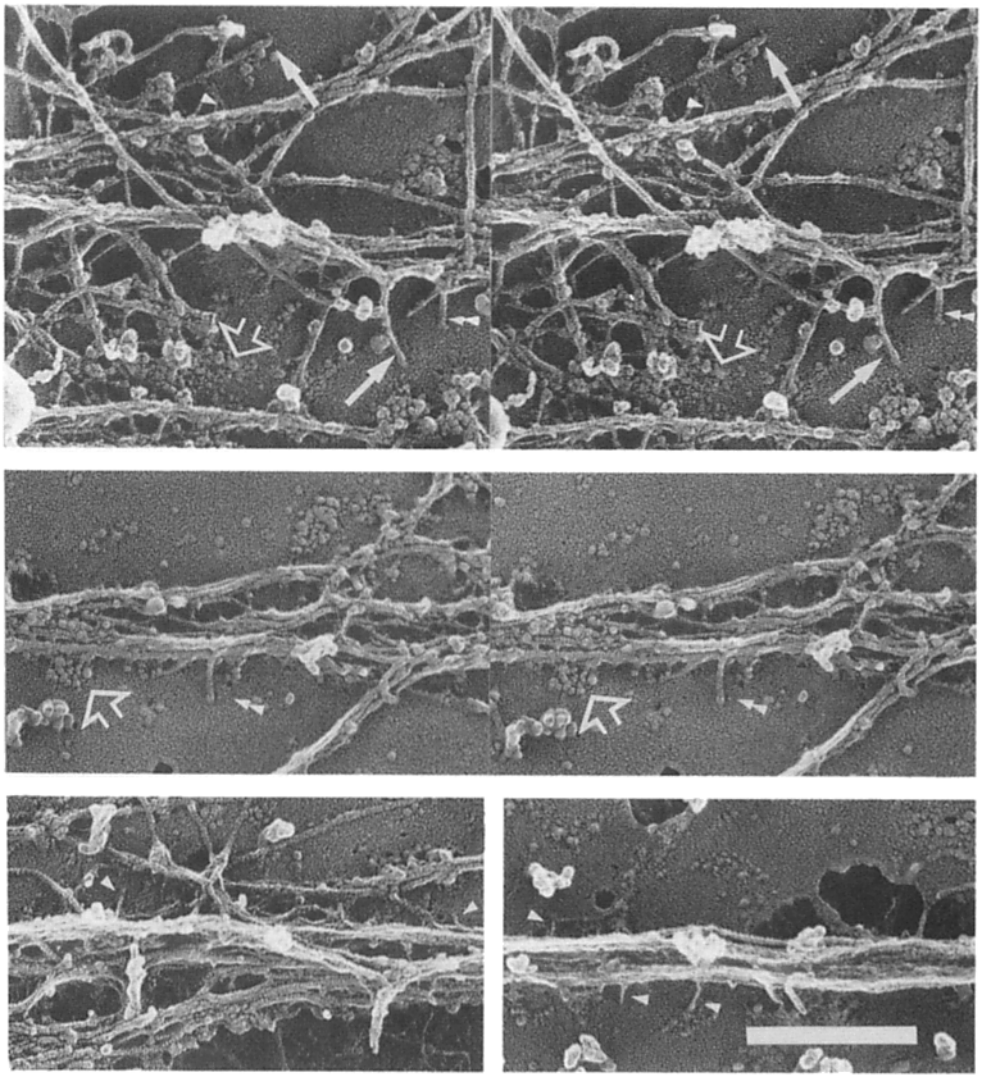

Figure 4. Short filaments run perpendicularly from the microfilament bundle to the membrane. These micrographs (upper and middle are stereo pairs) show two types of short filaments that link microfilament bundles to the membrane. One type of short filament (*dual arrowheads*) has a diameter of ~8.4 nm (without correction for ~1.2 nm of platinum) and the periodic banding typical of actin microfilaments. The second type of short filament (*arrowheads*) is only ~4 nm in diameter and is smooth. In addition, some single microfilaments seem to terminate directly on the plasmalemma (*arrow*). Type I aggregates of particles can be seen where they extend laterally from the microfilament bundles (*open arrows*). Bar, 0.25 μm.

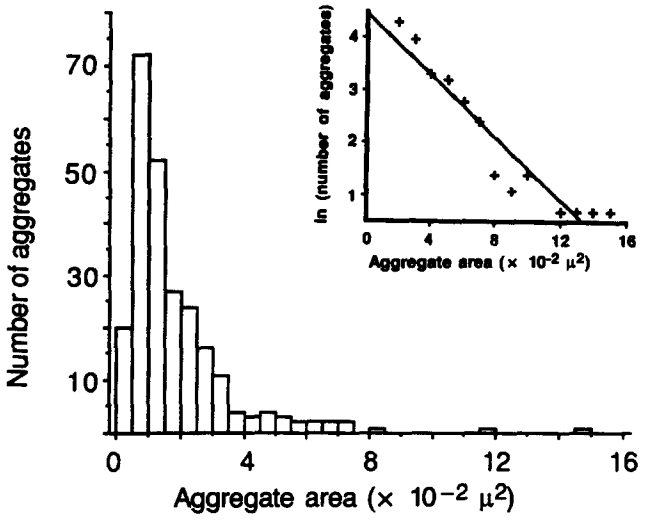

Figure 5. Large type I aggregates are less common than small aggregates. Type I aggregates have a wide range of sizes, and larger aggregates are progressively less common. The number of type I aggregates larger than 2×10^{-4} μm^2 in area decreases exponentially with size, so a plot of *ln* (number of aggregates) vs aggregate area fits a straight line (*inset*). This suggests that particles making up the aggregate interact only with their nearest neighbors, and that formation of larger aggregates is noncooperative.

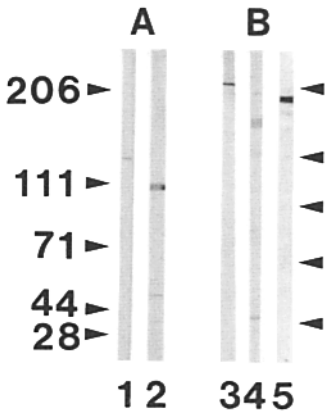

Figure 6. Specificity of antibodies assayed by immunoblotting. Tails of *Xenopus* tadpoles were dissected, boiled in sample buffer, and separated by SDS-PAGE in 10% (*A*) or 5–15% gradients (*B*) of polyacrylamide. After transfer to nitrocellulose paper, strips were incubated with antibodies followed by ^{125}I-protein A and visualized by autoradiography (lanes *2* and *3*), or by anti-antibodies coupled to HRP and visualized by a colorimetric reaction (lanes *1*, *4*, and *5*). (Lane *1*) mAb anti-vinculin labels a band at 127 kD, as expected (20). (Lane *2*) Affinity-purified rabbit anti-α-actinin labels bands at 105 and 50 kD. The latter is probably a proteolytic fragment of α-actinin (36, 54). (Lane *3*) Affinity-purified rabbit anti-talin labels a band at 210 kD, as expected (13). (Lane *4*) Affinity-purified rabbit antibody to the COOH-terminal sequence of β_1-integrin labels bands at 150 and 30 kD. The broad anti-integrin band at 150 kD may be indicative of multiple glycosylation sites (42); the smaller band is probably a COOH-terminal breakdown product. (Lane *5*) Affinity-purified rabbit anti-filamin labels a band at 190 kD, similar in size to the NH_2-terminal, actin-binding fragment of filamin (30). Arrowheads show the positions of standard proteins, as indicated in the left margin. These results indicate that the antibodies reacted specifically with the respective antigens or their proteolytic fragments in *Xenopus* extracts.

gregates could be fitted by a single exponential (Fig. 5). This pattern suggests that the binding of additional units to an aggregate is independent of the size of the aggregate (cf., reference 19), which in turn implies that aggregates could be assembled by independent addition of their component structures.

In addition to the type I aggregates that underlay all stress fibers at focal contacts, we observed other aggregates of cytoplasmic particles in our preparations (Fig. 2, *curved arrows*). The particles comprising these structures resembled those of type I aggregates, but the aggregates themselves were smaller in area ($3.7 \pm 1.9 \times 10^{-3}$ μm^2, range = 1.3–9.5; 32 aggregates from eight fields in two experiments) than type I aggregates, were circular rather than elongated, were not organized into linear arrays, and often were located between recognizable focal contacts. We refer to these as "type II aggregates." Considering their distinctive distribution, we believe that type II aggregates are not directly involved in the interactions between actin microfilaments and the membrane.

Except for the two types of particle aggregates and occasional areas of coated membrane and coated vesicles (e.g., Fig. 1 *c*; also visible in Fig. 9 *A*), the membrane between microfilament bundles was smooth. Tears in the membrane were common, however. These are probably due to stress during freeze-etching to a membrane already weakened by shearing, but we were unable to eliminate them even with glutaraldehyde or glutaraldehyde-acrolein fixation and the slow, controlled rates of etching that we used. Similar membrane defects appear in micrographs of replicated ventral membrane published elsewhere (e.g., references 49, 59).

We also observed two types of short filaments, oriented perpendicular to the microfilament bundles, that appeared to connect microfilaments and the membrane at focal contacts (Fig. 4). The thicker type of short filament (e.g., Fig. 4, *double arrowhead*) had a diameter of 8.4 ± 1.3 nm (mean ± SD, 12 filaments from six experiments; uncorrected for Pt coat of 1.2 nm), a length of 60 ± 21 nm, and showed a platinum repeat of 5.8 ± 0.4 nm (six filaments from two experiments). Although these were probably actin microfilaments, they were distinguishable from single actin microfilaments that branched from a bundle and angled towards the membrane (e.g., Fig. 4, *white arrows*) because they exited the microfilament bundle at a wide angle and were shorter and less variable in length. The second type of filament was thinner (4.1 ± 0.9 nm, 12 filaments from six experiments), shorter (31 ± 9 nm), and always appeared smooth (e.g., Fig. 4, *single arrowheads*). Neither type of short filament was abundant and many focal contacts did not appear to contain either structure.

Immunocytochemical Studies of Proteins of Focal Contacts

Our ultrastructural studies suggested that type I aggregates are the structures mediating the attachment of microfilaments to the membrane at focal contacts. We therefore used immunocytochemical methods to determine whether these aggregates contained proteins typical of focal contacts. We used antibodies that have been characterized previously in other species (6, 43, 62, 68), and confirmed that each bound an antigen with the appropriate molecular weight in extracts of *Xenopus* muscle (Fig. 6). Before using these antibodies to localize their respective antigens at the ultrastructural level, we tested their ability to label focal contacts and actin filaments by immunofluorescence. As expected, vinculin and talin were concentrated at focal contacts, but α-actinin and filamin were present both at focal contacts and elsewhere

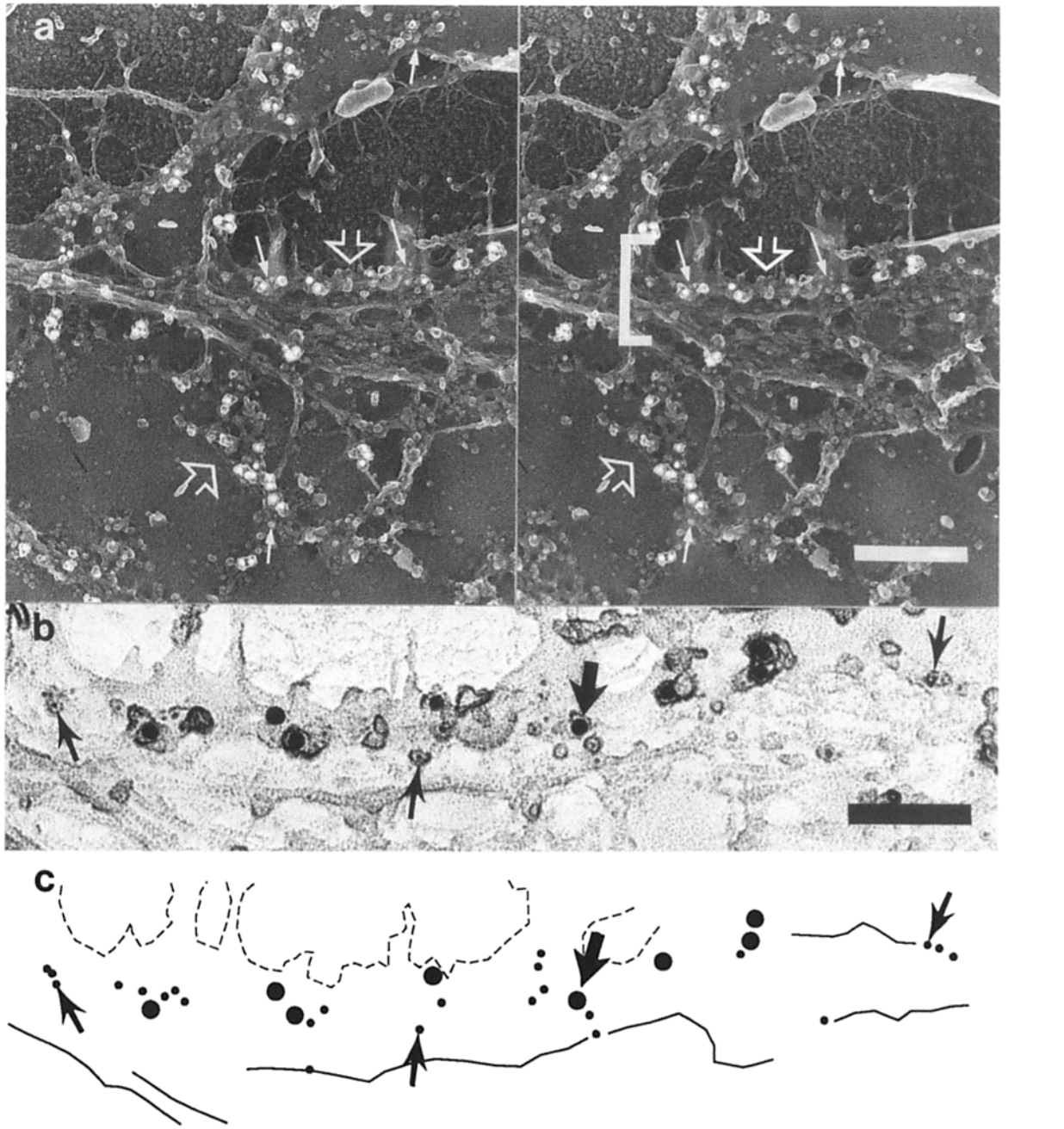

Figure 7. Stereo pair of focal contact labeled with anti-vinculin and anti-talin. After shearing, this sample was double labeled with a mouse antibody against vinculin (revealed by 5-nm colloidal gold particles) and with a rabbit antibody against talin (revealed by 15-nm colloidal gold particles). Although the smaller particles are difficult to see, the large difference in sizes made it easy to compare the distributions of the two markers. (*a*) Labeling by both antibodies occurs intermittently along the terminal region of the microfilaments. Labeling of vinculin (5-nm gold particles, *fine arrows*) and talin (15-nm gold particles, no arrows) in particle aggregates is clearest where the aggregates extended beyond the microfilament bundles (*open arrows*). This stereo micrograph of a relatively large area is shown at medium magnification. (*b*) Enlargement of the area to the right of the bracket in *a*. The 5-nm particles of colloidal gold are more easily seen here, without photographic reversal, especially as most are surrounded by small "haloes" due to bound protein and applied platinum. (Those particles that lack a halo were probably protected from the beam of platinum by surrounding structures). (*c*) Tracing of the micrograph shown in *b* indicates the positions of all the gold particles (15 nm, *large dots*; 5 nm, *small dots*). The thick lines represent actin microfilaments; the thin dashed lines represent an edge of the membrane fragment. Arrows indicate the same location in *b* and *c*. These results show that vinculin and talin codistribute in type I aggregates. Bars: (*a*) 0.25 μm; (*b* and *c*) 0.1 μm.

along bundles of actin microfilaments (not shown). Immunofluorescence data showed that β_1-integrin was present at focal contacts, but the binding of anti-integrin was limited unless actin microfilaments were first removed (e.g., during the shearing process or by alkaline extraction: Samuelsson, S. J., P. W. Luther, and R. J. Bloch, manuscript in preparation).

We used these antibodies in immunocytochemical experi-

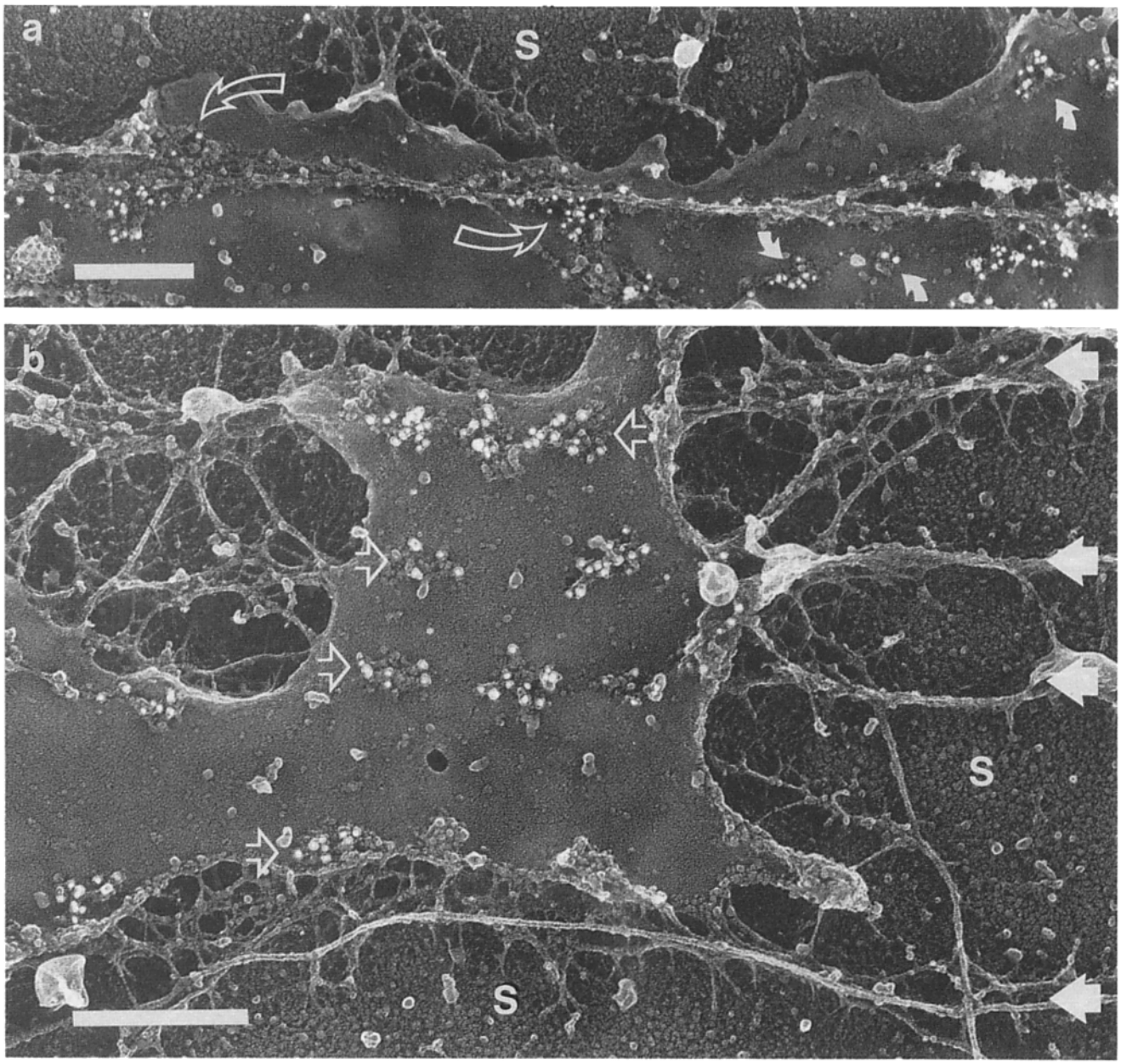

Figure 8. Focal contacts labeled with anti-β_1-integrin antibody. These samples were sheared, fixed, and labeled with a rabbit antibody to β_1-integrin followed by 10 nm colloidal gold probes. (*a*) Type I aggregates extending beyond a small microfilament bundle are labeled for integrin (*curved open arrow*). Type II particle aggregates away from the focal contact also label with integrin antibodies (*curved arrowheads*). (*b*) Linear extracellular matrix material (*thick arrows*) is seen near and below this fibroblast. Type I aggregates of particles align over these extracellular filaments. Anti-β_1-integrin antibodies label the particle aggregates (*open arrows*). *S*, substrate. Bars, 0.25 μm.

ments at the ultrastructural level. Vinculin (Figs. 7 and 9) and talin (Fig. 7) were both highly enriched at type I aggregates (Fig. 10). Stereoscopy showed that gold particles labeling talin and vinculin usually lay between the microfilaments and the membrane (not shown). In double labeling experiments, gold particles marking the two proteins lay very close to each other (Fig. 7, *b* and *c*). Thus, vinculin and talin codistributed in situ within type I aggregates. Antibodies to vinculin or talin did not label portions of microfilament bundles that were not close to the membrane (not shown).

Like labeling for vinculin and talin, labeling for β_1-integrin was present at type I aggregates (Fig. 8 *a*). Anti-β_1-integrin labeled the full extent of type I aggregates only when they were free of overlying microfilaments, however (e.g., Fig. 8 *b*), confirming immunofluorescence results (not shown). This suggests that access of antibodies to the COOH-terminal cytoplasmic sequence of β_1-integrin is blocked by overlying cytoskeletal structures (see Discussion; Samuelsson, S. J., P. W. Luther, and R. J. Bloch, manuscript in preparation).

Type II aggregates were also labeled by anti-β_1-integrin antibodies (Fig. 8 *a*, *curved arrowheads*) but were not labeled by antibodies to vinculin or α-actinin (Fig. 9, *c* and *d*, *arrows*), or by antibodies to talin (not shown). β_1-Integrin,

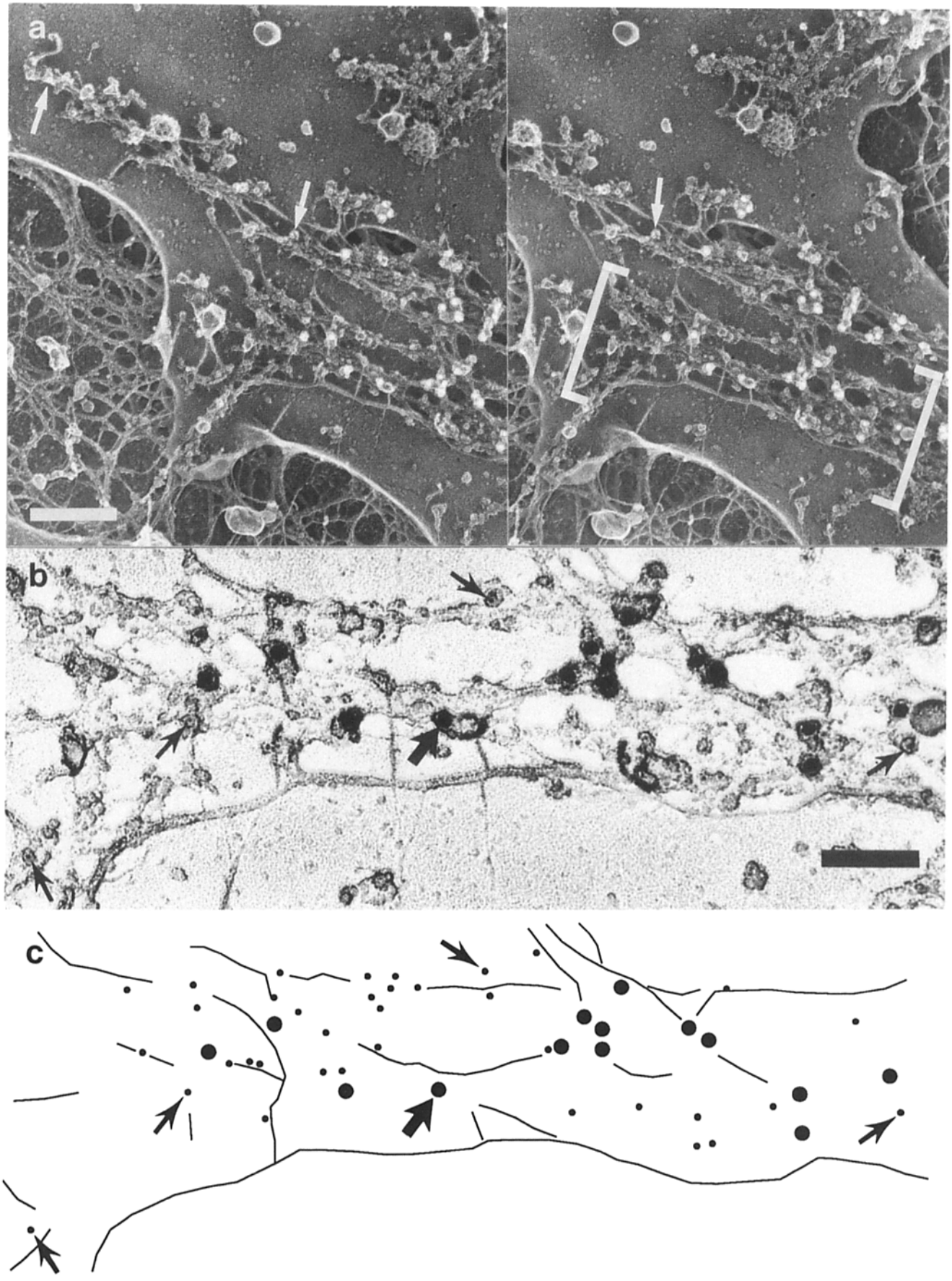

Figure 9.

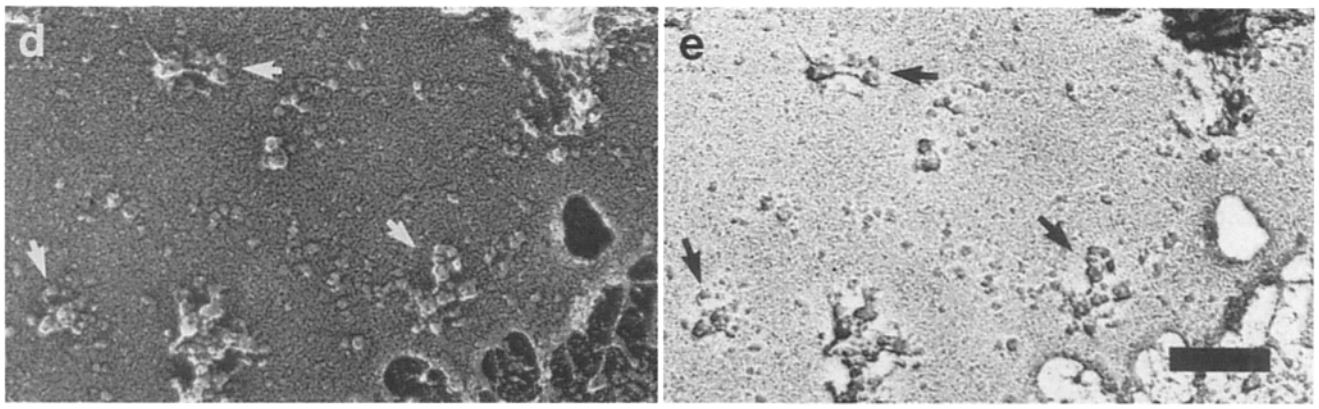

Figure 9. Stereo pair of a focal contact labeled with anti-vinculin and anti-α-actinin. This preparation was double labeled with mouse anti-vinculin (5-nm gold particles) and rabbit anti-α-actinin (15-nm gold particles). (*a*) Vinculin labeling was seen between the microfilaments and the membrane, where filaments obscure type I aggregates (e.g., *thin arrows*). In contrast, α-actinin labeling extended along the entire length of microfilaments. The type I aggregate seen at the upper right was not labeled with anti-α-actinin. (*b*) Enlargement of the area within the brackets in *a*, without photographic reversal (see Fig. 7), shows the relationship between 5-nm colloidal gold particles (e.g., *small arrows*) and 15-nm particles (e.g., *large arrow*). (*c*) Tracing of the micrograph shown in *b* indicates the positions of all the 15-nm (*large dots*) and 5-nm (*small dots*) gold particles. The thick lines represent actin microfilaments. Arrows indicate the same locations in *b* and *c*. (*d* and *e*) Type II aggregates (e.g., *arrows*) are not labeled with antibodies to vinculin and α-actinin, shown with (*d*) and without (*e*) photographic reversal. Bars: (*a*) 0.25 μm; (*b* and *c*) 0.10 μm; (*d* and *e*) 0.10 μm.

therefore, codistributes with vinculin and talin in type I aggregates, but occurs in the absence of these other proteins in type II aggregates.

Immunogold labeling for α-actinin (Fig. 9) and filamin (69; data not shown) appeared in stress fibers both at and near focal contacts. Stereoscopic views of focal contacts showed that this labeling was distributed around microfilaments (Fig. 9). In some samples, anti-α-actinin and anti-filamin antibodies labeled type I aggregates even when no actin microfilaments were evident. Quantitation of gold particles in such areas showed that type I aggregates were labeled by anti-α-actinin, or anti-filamin more sparsely than by anti-vinculin, anti-talin, or anti-β_1-integrin (Fig. 10).

Our labeling procedures were specific. The antibodies we used gave distinctive patterns of labeling, and only a few gold particles were seen following labeling with a control mouse antibody (MOPC 21: Fig. 10) or with preimmune rabbit serum (not shown). This control labeling was random and not associated specifically with aggregates of membrane particles.

Extracellular Matrix at Focal Contacts

Extracellular matrix associated with *Xenopus* fibroblasts was easily distinguished from the denatured collagen substrate in our replicas (Fig. 8). In some samples we found type I aggregates, labeled with anti-β_1-integrin, aligned above bundles of extracellular filaments (Fig. 8 *b*, *thick arrow*). These results suggest that, like integrin-rich structures in other cells (1, 61), type I aggregates are associated with extracellular matrix.

Discussion

We isolated membranes from cultured *Xenopus* fibroblasts and used quick-freeze, deep-etch, rotary replication to investigate the interface between microfilaments and the cytoplasmic surface of the membrane at focal contacts. Although several ultrastructural techniques have been used to examine focal contacts (e.g., 8, 25, 50, 64, 66), our shearing and quick-freezing procedures are the first to give a wide view of ventral membrane and simultaneously to preserve the three-dimensional relationship between microfilaments and the membrane that is seen at focal contacts in intact cells

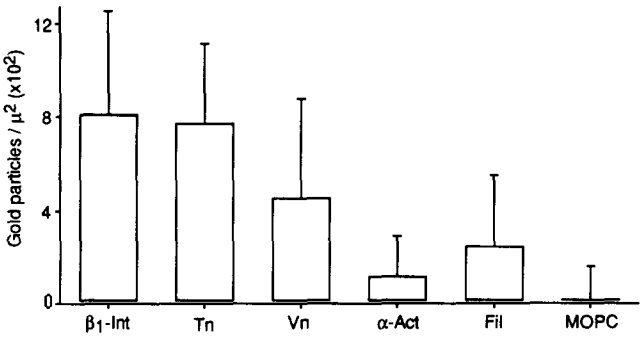

Figure 10. Bar graph comparing density of immunolabeling at membrane-associated particle aggregates. Gold particles overlying clearly exposed type I aggregates where counted by hand, whereas areas of aggregates were measured with a digitizing tablet. The concentrations of β_1-integrin and talin at the aggregates were three to four times higher than the concentration of α-actinin and filamin, and these differences were significant ($P < .05$, multiple correlation rank sum test). Vinculin labeling was significantly less than labeling for β_1-integrin and talin, but not significantly greater than labeling for filamin. Labeling by the control antibody, MOPC 21, was absent at 68 of 73 particle aggregates; labeling by nonimmune rabbit IgG was also extremely infrequent (not shown). The large standard deviation in samples labeled by MOPC 21 was caused by a cluster of 11 gold particles associated with a single aggregate. Nevertheless, labeling by MOPC 21 was significantly lower than that for filamin and vinculin ($P < .001$). though not for α-actinin ($P > .05$). When the data are analyzed without including the cluster of 11 gold particles in the MOPC 21 sample, the difference between MOPC 21 and α-actinin is highly significant ($P < .001$).

(e.g., 2, 16, 28, 32, 44, 49, 56, 65). These techniques reveal distinctive aggregates of membrane-associated particles that link microfilaments to the membrane, and show that vinculin, talin, and integrin are concentrated in these aggregates.

Actin-Membrane Interactions

Our results show that most of the sites where microfilaments attach to the membrane contain elongated aggregates of particles that project from the inner surface of plasma membrane. These type I aggregates are found intermittently along the terminal few microns of microfilament bundles. As they extend from the membrane and seem to contact microfilaments at several sites, these aggregates appear to mediate multiple lateral attachments of microfilaments to the membrane at focal contacts. Consistent with this idea, type I aggregates contain at least three proteins typical of focal contacts—vinculin, talin, and β_1-integrin—that are believed to link microfilaments to the cytoplasmic face of the plasma membrane. Thus, type I aggregates are both the dominant membrane specialization at focal contacts and the structure in which the major proteins of focal contacts are located.

In addition to the type I aggregates, two other structures may contribute to microfilament-membrane interactions at focal contacts. (*a*) Short actin-like filaments extend perpendicularly from the main body of the filament bundle and appear to attach directly to the membrane. The discrepancy between the diameters of the short filaments (8.4 nm) and single microfilaments located further from the membrane (10.3 nm) can be explained if replication of the former is partly obscured by the adjacent microfilament bundles. Our replicas do not reveal whether the short filaments insert directly into the bilayer, which could be facilitated by cytoskeleton lipid interactions (52, 67), or if they bind via proteins that are too small to be detected by replication (e.g., ponticulin: 72). (*b*) Actin-membrane attachments are also mediated by short, ~4-nm diam filaments that, unlike actin, show no periodicity of platinum decoration. These small filaments also appear to attach directly to the membrane. Similar filaments associated with actin have been described by others (31, 34, 63; Hartwig, J. H., P. A. Janmey, A. Rosen, M. Thelem, A. C. Nairn and A. Aderem. 1990. *J. Cell Biol.* 111:8*a*). α-Actinin, too, is approximately this size (36). These filaments were not labeled by any of the antibodies we used, however.

Aggregates of Membrane Particles

It is likely that integrin accounts in large part for the distinctive appearance of the particle aggregates at focal contacts. With the exception of overall size, the ultrastructure of type I aggregates, which contain integrin, vinculin, and talin, is identical to that of type II aggregates, which contain integrin but not vinculin or talin. Thus, despite their large size, vinculin and talin are not apparent as distinctive structures at the cytoplasmic aspect of focal contacts. This implies that either these proteins do not have the distinctive shape in situ that they assume when isolated (45), or that individual proteins are obscured within the complex organization of the particle aggregates.

Type II aggregates are composed of several individual particles, consistent with observations that purified integrin can aggregate (48). Although integrin almost certainly accounts in part for the appearance of the particles, replication of the small cytoplasmic domain of integrin in type II aggregates would not be expected to produce projections of the size that we see (48). Platinum decoration could conceivably enlarge them. Alternatively, the 50-kD integrin-associated protein (11) or macromolecules other than vinculin and talin may be present at these sites and contribute to the cytoplasmic aspect of integrin aggregates.

Our results clearly show that vinculin and talin occur in type I particle aggregates, where they could mediate the association of actin with the cytoplasmic tail of integrin (14, 35, 42, 46, 60). The proximity of actin filaments to β_1-integrin is suggested by our observation that antibodies to the cytoplasmic tail of β_1-integrin did not label that protein when overlying actin filaments are present. In double labeling experiments, we also found that binding of anti-vinculin antibodies reduced the ability of anti-β_1-integrin antibodies to label type I, but not type II, aggregates (S. Samuelsson, unpublished observations). These observations are consistent with the idea that vinculin and actin microfilaments are closely associated with β_1-integrin at focal contacts.

In contrast to vinculin and talin, α-actinin and filamin appear to be less prominent components of type I aggregates. Quantitative estimates of the density of these proteins must be interpreted with caution because of the possibilities of nonsaturating labeling conditions, steric hindrance, antigen loss during shearing, differences in antibody affinities, and the presence of isoforms not recognized by our antibodies. Nonetheless, because both α-actinin and filamin distribute along bundles of actin filaments and do not appear preferentially at type I aggregates, these proteins are more likely to be involved in organizing the filaments into bundles than in attaching them to the plasma membrane.

Although focal contacts have been examined by others using replication methodology, the ultrastructural elements that we report were not previously described. Feltkamp et al. (25) used "wet cleaving" to expose the cytoplasmic surface of focal contacts and then processed their samples by critical point drying. They observed immunogold labeling of vinculin and talin at focal contacts but were unable to resolve the particulate structures containing these proteins. In the chick fibroblasts they examined, labeling for vinculin and talin was usually continuous and not intermittent, as we report for *Xenopus* fibroblasts. This difference may be due to species or tissue variation. Nermut et al. (49) employed "lysis-squirting" followed by either critical point drying or plunge-freezing in liquid nitrogen to study the cytoplasmic surface of focal contacts in rat fibroblasts. They showed that vinculin was distributed along microfilaments and associated with particulate material, but their methods did not preserve the three-dimensional organization of the focal contact. Our ability to preserve this organization is probably due to careful adjustment of the amount of water on the samples before rapid freezing on a metal mirror (33, 55, 57; reviewed in 24, 29).

Significance

The factors that control the growth of actin microfilaments at the cell periphery and the distribution of integrin in the plasma membrane are still poorly understood. Actin microfilaments grow preferentially at their "barbed" ends. As these are also the ends that attach at focal contacts, it has

been difficult to understand how microfilaments in stress fibers elongate. Our observation that bundles of microfilaments attach laterally to the membrane at focal contacts suggests that the barbed ends may be free to elongate without first detaching. Chia et al. (18) recently reported that ponticulin mediates lateral attachment of microfilaments to the plasma membrane in *Dictyostelium*, allowing growth at both the pointed and the barbed ends. Although we cannot rule out the possibility that an interaction between actin and the membrane occurs at the ends, our data suggest that lateral attachments are sufficient to anchor microfilaments.

Cells contain significant amounts of integrin that is mobile in the plasma membrane (23) and that redistributes during the formation of new attachment sites (e.g., references 17, 22, 58, 66). The integrin in type I aggregates of *Xenopus* fibroblasts is probably immobile, as observed at focal contacts in other cells (23; see also reference 27). The type II aggregates, which contain integrin but are not associated with the cytoskeleton, may contribute to the mobile integrin fraction, however. Although the relationship between type I and type II aggregates remains unclear, it seems possible the two are in equilibrium, and that the formation of type I aggregates may be triggered by binding of type II aggregates of integrin to extracellular proteins and subsequent signaling events (see, e.g., reference 38). With this possibility in mind, we are continuing our immunocytochemical studies to characterize the peripheral membrane proteins associated with type I and type II aggregates of integrin in *Xenopus* fibroblasts.

Our research is supported by grants from the National Institutes of Health to Dr. Luther (NS27171), Dr. Pumplin (NS15513), and Dr. Bloch (NS17282) and by grants from the Muscular Dystrophy Association to Drs. Pumplin and Bloch.

Received for publication 18 July 1992 and in revised form 28 April 1993.

References

1. Albelda, S. M., and C. A. Buck. 1990. Integrins and other cell adhesion molecules. *FASEB (Fed. Am. Soc. Exp. Biol.) J.* 4:2868–2880.
2. Abercrombie, M., J. E. M. Heaysman, and S. M. Pegrum. 1971. The locomotion of fibroblasts in culture. IV. Electron microscopy of the leading lamella. *Exp. Cell Res.* 67:359–367.
3. Anderson, M. J., M. W. Cohen, and E. Zorychta. 1977. Effects of innervation on the distribution of acetylcholine receptors on cultured muscle cells. *J. Physiol. (Lond.).* 268:731–756.
4. Avnur, Z., and B. Geiger. 1981. Substrate attached membranes of cultured cells. Isolation and characterization of ventral cell membrane and the associated cytoskeleton. *J. Mol. Biol.* 153:361–379.
5. Beckerle, M. C. 1986. Identification of a new protein localized at sites of cell-substrate adhesion. *J. Cell Biol.* 103:1679–1687.
6. Bloch, R. J., and Z. W. Hall. 1983. Cytochemical components of the vertebrate neuromuscular junction: vinculin, α-actinin and filamin. *J. Cell Biol.* 97:217–223.
7. Bloch, R. J., M. Velez, J. G. Krikorian, and D. Axelrod. 1989. Microfilaments and actin-associated proteins at sites of substrate attachment in acetylcholine receptor clusters of cultured rat myotubes. *Exp. Cell Res.* 182:583–596.
8. Brands, R., A. de Boer, C. A. Feltkamp, and E. Roos. 1990. Disintegration of adhesion plaques in chicken embryo fibroblasts upon Rous sarcoma virus-induced transformation: different dissociation rates for talin and vinculin. *Exp. Cell Res.* 186:138–148.
9. Bretscher, A., and K. Weber. 1980. Fimbrin, a new microfilament-associated protein present in microvilli and other cell surface structures. *J. Cell Biol.* 86:335–340.
10. Bridgman, P. C., and T. S. Reese. 1984. The structure of cytoplasm in directly frozen cultured cells. I. Filamentous meshworks and the cytoplasmic ground substance. *J. Cell Biol.* 99:1655–1668.
11. Brown, E., L. Hooper, T. Ho, and H. Gresham. 1990. Integrin-associated protein: a 50-kD plasma membrane antigen physically and functionally associated with integrin. *J. Cell Biol.* 111:2785–2794.
12. Burnett, W. N. 1981. Western blotting: electrophoretic transfer of proteins from sodium dodecyl sulfate-polyacrylamide gels to unmodified nitrocellulose and radiographic detection with antibody and radioiodinated protein. *Anal. Biochem.* 112:195–203.
13. Burridge, K., and L. Connell. 1983. A new protein of adhesion plaques and ruffling membranes. *J. Cell Biol.* 97:359–367.
14. Burridge, K., and P. Mangeat. 1984. An interaction between vinculin and talin. *Nature (Lond.).* 308:744–746.
15. Burridge, K., K. Fath, T. Kelly, G. Nuckolls, and C. Turner. 1988. Focal adhesions: transmembrane junctions between the extracellular matrix and the cytoskeleton. *Annu. Rev. Cell Biol.* 4:487–525.
16. Chen, W.-T., and S. J. Singer. 1982. Immunoelectron microscopic studies of the sites of cell-substratum and cell–cell contacts in cultured fibroblasts. *J. Cell Biol.* 95:205–222.
17. Chen, W.-T., E. Hasegawa, T. Hasegawa, C. Weinstock, and K. M. Yamada. 1985. Development of cell surface linkage complexes in cultured fibroblasts. *J. Cell Biol.* 100:1103–1114.
18. Chia, C. P., A. Shariff, S. A. Savage, and E. J. Luna. 1993. The integral membrane protein, ponticulin, acts as a monomer in nucleating actin assembly. *J. Cell Biol.* 120:909–922.
19. Cohen, S. A., and D. W. Pumplin. 1979. Clusters of intramembrane particles associated with binding sites for α-bungarotoxin in cultured chick myotubes. *J. Cell Biol.* 82:494–515.
20. Coutu, M. D., and S. W. Craig. 1988. cDNA-derived sequence of chicken embryo vinculin. *Proc. Natl. Acad. Sci. USA.* 85:8535–8539.
21. Damsky, C. H., K. A. Knudsen, D. Bradley, C. A. Buck, and A. F. Horwitz. 1985. Distribution of the cell substratum attachment (CSAT) antigen on myogenic and fibroblastic cells in culture. *J. Cell Biol.* 100: 1528–1539.
22. Dejana, E., S. Colella, G. Conforti, M. Abbadini, M. Gaboli, and P. C. Marchisio. 1988. Fibronectin and vitronectin regulate the organization of their Arg-Gly-Asp adhesion receptors in cultured human endothelial cells. *J. Cell Biol.* 107:1215–1223.
23. Duband, J.-L., G. H. Nuckolls, A. Ishihara, T. Hasegawa, K. M. Yamada, J. P. Thiery, and K. Jacobson. 1988. Fibronectin receptor exhibits high lateral mobility in embryonic locomoting cells but is immobile in focal contacts and fibrillar streaks in stationary cells. *J. Cell Biol.* 107: 1385–1396.
24. Escaig, J. 1982. Ultra-rapid freezing of cells and cellular material: a review of methods. *Proc. Tenth Intl. Cong. Elec. Microsc.* 3:169–176.
25. Feltkamp, C. A., M. A. Pijnenburg, and E. Roos. 1991. Organization of talin and vinculin in adhesion plaques of wet-cleaved chicken embryo fibroblasts. *J. Cell Sci.* 100:579–587.
26. Geiger, B. 1979. A 130K protein from chicken gizzard: its localization at the termini of microfilament bundles in cultured chicken cells. *Cell.* 18:193–205.
27. Geiger, B., Z. Avnur, and J. Schlessinger. 1982. Restricted mobility of membrane constituents in cell-substrate contacts of chicken fibroblasts. *J. Cell Biol.* 93:495–500.
28. Geiger, B., K. T. Tokuyasu, A. H. Dutton, and S. J. Singer. 1980. Vinculin, an intracellular protein localized at specialized sites where microfilament bundles terminate at cell membranes. *Proc. Natl. Acad. Sci. USA.* 77:4127–4131.
29. Gilkey, J. C., and A. Staehelin. 1986. Advances in ultrarapid freezing for the preservation of cellular ultrastructure. *J. Elect. Microsc. Tech.* 3: 177–210.
30. Gorlin, J. B., R. Yamin, S. Egan, M. Stewart, T. P. Stossel, D. J. Kwiatkowski, and J. H. Hartwig. 1990. Human endothelial actin-binding protein (ABP-280, nonmuscle filamin): a molecular leaf spring. *J. Cell Biol.* 111:1089–1105.
31. Heath, J. P., and F. Bard. 1987. Deep etching of rapidly frozen cytoskeleton of motile fibroblasts. *In* Proceedings of the 45th Annual Meeting of the Electron Microscopy Society of America. G. W. Bailey, editor. San Francisco Press, Inc., San Francisco. 900–901.
32. Heath, J. P., and G. A. Dunn. 1978. Cell-to-substratum contacts of chick fibroblasts and their relation to the microfilament system. A correlated interference-reflexion and high-voltage electron-microscope study. *J. Cell Sci.* 29:197–212.
33. Heuser, J. E., and M. W. Kirschner. 1980. Filament organization revealed in platinum replicas of freeze-dried cytoskeletons. *J. Cell Biol.* 86: 212–234.
34. Hirokawa, N., and L. Tilney. 1982. Interactions between actin filaments and between actin filaments and membranes in quick-frozen and deeply etched hair cells of the chick ear. *J. Cell Biol.* 95:249–261.
35. Horwitz, A., K. Duggan, C. Buck, M. C. Beckerle, and K. Burridge. 1986. Interaction of plasma membrane fibronectin receptor with talin—a transmembrane linkage. *Nature (Lond.).* 320:531–533.
36. Imamura, M., T. Endo, M. Kuroda, T. Tanaka, and T. Masaki. 1988. Substructure and higher structure of chicken smooth muscle α-actinin molecule. *J. Biol. Chem.* 263:7800–7805.
37. Jones, K. W., and T. R. Elsdale. 1963. The culture of small aggregates of amphibian embryonic cells in vitro. *J. Embryol. Exp. Morphol.* 11: 135–154.
38. Juliano, R. L., and S. Haskill. 1993. Signal transduction from the extracellular matrix. *J. Cell Biol.* 120:577–585.

39. Laemmli, U. K. 1970. Cleavage of structural proteins during the preassembly of bacteriophage T4. *Nature (Lond.).* 227:680–685.
40. Lazarides, E., and K. Burridge. 1975. α-Actinin: immunofluorescent localization of a muscle structural protein in nonmuscle cells. *Cell.* 6: 189–198.
41. Luther, P. W., and R. J. Bloch. 1989. Formaldehyde-amine fixatives for immunocytochemistry of cultured *Xenopus* myocytes. *J. Histochem. Cytochem.* 37:75–82.
42. Maher, P. A., and S. J. Singer. 1988. An integral membrane protein antigen associated with the membrane attachment sites of actin microfilaments is identified as an integrin β-chain. *Mol. Cell. Biol.* 8:564–570.
43. Marcantonio, E. E., and R. O. Hynes. 1988. Antibodies to the conserved cytoplasmic domain of the integrin β_1 subunit react with proteins in vertebrates, invertebrates, and fungi. *J. Cell Biol.* 106:1765–1772.
44. Maupin, P., and T. D. Pollard. 1983. Improved preservation and staining of HeLa cell actin filaments, clathrin-coated membranes and other cytoplasmic structures by tannic acid-glutaraldehyde-saponin fixation. *J. Cell Biol.* 96:51–62.
45. Molony, L., and K. Burridge. 1985. Molecular shape and self-association of vinculin and metavinculin. *J. Cell Biochem.* 29:31–36.
46. Muguruma, M., S. Matsumura, and T. Fukazawa. 1990. Direct interactions between talin and actin. *Biochem Biophys. Res. Commun.* 171: 1217–1223.
47. Neff, N. T., C. Lowrey, C. Decker, A. Tovar, C. Damsky, C. Buck, and A. F. Horwitz. 1982. A monoclonal antibody detaches embryonic skeletal muscle from extracellular matrices. *J. Cell Biol.* 95:654–666.
48. Nermut, M. V., N. M. Green, P. Eason, S. S. Yamada, and K. M. Yamada. 1988. Electron microscopy and structural model of human fibronectin receptor. *EMBO (Eur. Mol. Biol. Organ.) J.* 7:4093–4099.
49. Nermut, M. V., P. Eason, E. M. A. Hirst, and S. Kellie. 1991. Cell/substratum adhesions in RSV-transformed rat fibroblasts. *Exp. Cell Res.* 193:382–397.
50. Nicol, A., M. V. Nermut, A. Doeinck, H. Robenek, C. Wiegand, and B. M. Jockusch. 1987. Labeling of structural elements at the ventral plasma membrane of fibroblasts with the immunogold technique. *J. Histochem. Cytochem.* 35:499–506.
51. Nieuwkoop, P. D., and J. Faber. 1967. Normal Table of *Xenopus laevis* (Daudin). Elsevier/North-Holland Biomedical Press, Amsterdam. 252 pp.
52. Niggli, V., L. Sommer, J. Brunner, and M. M. Burger. 1990. Interaction *in situ* of the cytoskeletal protein vinculin with bilayers studied by introducing a photoactivatable fatty acid into living chicken embryo fibroblasts. *Eur. J. Biochem.* 187:111–117.
53. Otey, C., F. M. Pavalko, and K. Burridge. 1990. An interaction between α-actinin and the β_1-integrin subunit in vitro. *J. Cell Biol.* 111:721–729.
54. Pavalko, F. M., and K. Burridge. 1991. Disruption of the actin cytoskeleton after microinjection of proteolytic fragments of α-actinin. *J. Cell Biol.* 114:481–491.
55. Phillips, T. E., and A. F. Boyne. 1984. Liquid nitrogen-based quick freezing: experiences with bounce-free delivery of cholinergic nerve terminals to a metal surface. *J. Elect. Microsc. Techn.* 1:9–29.
56. Pumplin, D. W. 1989. Acetylcholine receptor clusters of rat myotubes have at least three domains with distinctive cytoskeletal and membrane components. *J. Cell Biol.* 109:739–753.
57. Pumplin, D. W., P. W. Luther, S. J. Samuelsson, J. A. Ursitti, and J. Strong. 1990. Quick-freeze, deep-etch replication of cells in monolayers. *J. Elect. Microsc. Techn.* 14:342–347.
58. Regen, C. M., and A. F. Horwitz. 1992. Dynamics of β_1 integrin-mediated adhesive contacts in motile fibroblasts. *J. Cell Biol.* 119: 1347–1359.
59. Rothberg, K. B., J. E. Heuser, W. C. Donzell, Y.-S. Ying, J. R. Glenney, and R. G. W. Anderson. 1992. Caveolin, a protein component of caveolae membrane coats. *Cell.* 68:673–682.
60. Ruhnau, K., and A. Wegner. 1988. Evidence for direct binding of vinculin to actin filaments. *FEBS (Fed. Eur. Biochem. Soc.) Lett.* 228:105–108.
61. Ruoslahti, E. 1988. Fibronectin and its receptor. *Annu. Rev. Biochem.* 57:375–413.
62. Saga, S., M. Hamaguchi, M. Hoshino, and K. Kojima. 1985. Expression of meta-vinculin associated with differentiation of chicken embryonal muscle cells. *Exp. Cell Res.* 156:45–56.
63. Schliwa, M., and J. van Blerkom. 1981. Structural interaction of cytoskeletal components. *J. Cell Biol.* 90:222–235.
64. Semich, R., and H. Robenek. 1990. Organization of the cytoskeleton and the focal contacts of bovine aortic endothelial cells cultured on type I and III collagen. *J. Histochem. Cytochem.* 38:59–67.
65. Singer, I. 1979. The fibronexus: a transmembrane association of fibronectin-containing fibers and bundles of 5 nm microfilaments in hamster and human fibroblasts. *Cell.* 16:675–685.
66. Singer, I. I., D. M. Kazazis, and S. Scott. 1989. Scanning electron microscopy of focal contacts on the substratum attachment surface of fibroblasts adherent to fibronectin. *J. Cell Sci.* 93:147–154.
67. St-Onge, D., and C. Gicquaud. 1990. Research on the mechanism of interaction between actin and membrane lipids. *Biochem. Biophys. Res. Commun.* 167:40–47.
68. Turner, C. E., J. R. Glenney, Jr., and K. Burridge. 1990. Paxillin: a new vinculin-binding protein present in focal adhesions. *J. Cell Biol.* 111: 1059–1068.
69. Wang, K., J. F. Ash, and S. J. Singer. 1975. Filamin, a new high-molecular-weight protein found in smooth muscle and non-muscle cells. *Proc. Natl. Acad. Sci. USA.* 72:4483–4486.
70. Wildhaber, L., H. Gross, and H. Moor. 1982. The control of freeze-drying with deuterium oxide (D_2O). *J. Ultrastruct. Res.* 80:367–373.
71. Wilkins, J. A., and S. Lin. 1986. A re-examination of the interaction of vinculin with actin. *J. Cell Biol.* 102:1085–1092.
72. Wuestehube, L. J., and E. J. Luna. 1987. F-actin binds to the cytoplasmic surface of ponticulin, a 17-kD integral glycoprotein from *Dictyostelium discoideum* plasma membranes. *J. Cell Biol.* 105:1741–1751.